A NOVEL METHOD TO INCREASE ENERGY DENSITY OF PERMANENT MAGNET MACHINE BASED ON MULTI-PHYSICAL FIELD ANALYSIS

Qingchun ZHENG[1], Yangyang ZHAO[2,3,4]*, Peihao ZHU[1]*, Sen WANG[3], Jingna LIU[1], Wenpeng MA[1], Xiang LI[1], Yinhong XIAO[1], Naixin WANG[1]

As an important component of all-electric aircraft, the main propulsion machine is developing towards high energy density, high efficiency and high fault tolerance. In order to improve the energy density of main propulsion machine for all-electric aircraft, a novel approach, which can be used for excellent performance improvement of electric machine of all-electric aircraft, is reported in this paper. The analytical formula of energy density is put forward and the design method of high energy density permanent magnet machine is presented. A high energy density machine with rated power of 30kW is designed, and the electromagnetic field simulation analysis, strength and stress structure verification, temperature field simulation analysis and multi-physical field coupling analysis are obtained. A prototype is developed, the experiment platform is established, and experiments are performed. The energy density of main propulsion machine designed is up to 21kW·N·m/kg^2, and the index is increased by 3.2 times. The optimal method based on the multi-physical field analysis can be also applied to other high energy density machines.

Keywords: All-electric aircraft, Permanent magnet machine, High energy density, Multi-physical field

1. Introduction

In recent years, with the global attention to the construction of ecological civilization and green energy, electric technology has ushered in new development opportunities. At present, many research institutes in the world are developing new electric aircraft, which plays an active role in promoting the development of general aviation industry. Electric aircraft usually takes new energy sources as power source, mainly including super capacitors, fuel cells and batteries, etc. By

[1]Tianjin Key Laboratory for Advanced Mechatronic System Design and Intelligent Control, School of Mechanical Engineering, Tianjin University of Technology, Tianjin, 300384, China.
[2]School of Computer Science, Tianjin University of Technology, Tianjin, 300384, China.
[3]School of Automation, Shenyang Institute of Engineering, Shenyang, 110136, China.
[4]Baoding Power Supply Company, Hebei Electric Power Company, State Grid Corporation of China, Baoding, 071000, China.
*E-mail: zhupeihao_gp@163.com, zhaoyangyangcn@163.com

driving electric machines to make propeller rotate at high speed, the aircraft can generate forward power and lift. There are some features for all-electric aircraft, such as high energy transmission efficiency, low carbon, environmental protection, low noise, low cost, simple structure and convenient maintenance. It has a great development prospect in the fields of tourism, flight experience, emergency and disaster relief, space photography, agricultural and forestry quality assurance.

Battery, electric machine and control system is the three key technologies of all-electric aircraft. Under the current level of battery energy density, the inexorable requirement of all-electric aircraft power system is small in size, light weight, big transmission output power and torque, so lightweight technology of main propulsion machine is one of the focuses on all-electric aircraft.

Experts and scholars have carried out special research on main propulsion system of electric aircraft. Evgeni Ganev pointed out that high performance electric drive system is one of development direction for electric aircraft in the future, in which permanent magnet machine will play a very important role. He proposed the idea of using toothless permanent magnet machine for main propulsion of electric aircraft and the cooling problem is considered in the research process [1]. Patrick Ragot used pro design software and sequential quadratic programming algorithm to optimize the design of solar powered aircraft machine, and analyzed the temperature field model by thermal circuit method [2]. The 55kW electric machine system developed by Dalibor Cervinka was successfully applied to the VUT 051 RAY electric aircraft, and the theoretical method to calculate the efficiency of electric machine system was presented [3]. Wenping Cao studies electric machine system theory of light electric aircraft. By comparing the fault-tolerant capacity, power density, efficiency, torque ripple, noise and other comprehensive factors of induction machine, reluctance machine and permanent magnet machine, it is concluded that permanent magnet machine is more suitable for main propulsion [4]. Philippe j. Masson studied the high power density superconducting machine for main propulsion of all-electric aircraft, and designed a 164kW, 585Nm, 28kg super power density and torque density machine with high air gap magnetic density [5]. However, many problems exist in the manufacturing process of superconducting machines, such as vacuum sealing of rotary infusion sealing device, winding manufacturing, coil detection and protection and cost, so it is not suitable for industrialization. Sukumar De has made some research on low-inductance axial flux brushless DC machine for light aircraft, and proposed a new research idea of main propulsion machine for electric aircraft [6]. Combined lumped parameter thermal analysis method with three-dimensional finite element thermal analysis method, Sang-taek Lee analyzed and tested temperature rise of the embedded permanent magnet synchronous machine. The experimental results were similar to the analysis results, which was conducive

to improving thermal performance of electric machine [7]. Zheng TAN optimized the structure of axial flux permanent magnet machine and proposed a CFD analysis of the three-dimensional heat. The cooling fan designed is conducive to heat dissipation [8]. James d. Widmer designed and studied the aluminum winding external rotor permanent magnet machine of solar main propulsion. Under the same electromagnetic performance, aluminum winding machine has more advantages in heat dissipation performance and cost [9]. Vadim Iosif studied high temperature and low voltage machines, studied the insulation of inorganic chemical materials in the winding, and applied thin ceramic coating on the winding to run at 500℃ to greatly improve the current density of machines [10].

Electric aircraft requires high power density, high torque density, small size, high efficiency and good cooling effect of main propulsion machine, among which high power density and torque density are even greater than efficiency, therefore this paper takes the energy density as an important key parameter in the design process. Conventional induction machines and ordinary permanent magnet machines have low energy density, not suitable for main propulsion.

In order to improve the energy density of main propulsion machine of electric aircraft, the comprehensive physical field technology should be considered. Therefore, the electromagnetic field, temperature field and mechanical field of main propulsion machine should be analyzed. To design a high energy density machine, firstly the design method of high energy density permanent magnet machine is presented. Then the electromagnetic simulation analysis, strength and stress verification and electromagnetic-temperature coupling analysis of PMSM are presented emphatically. Finally the experimental process and experimental data of the actual prototype are provided.

2. Design of high energy density permanent magnet machine

2.1 Energy density

According to the formulas of calculated power, potential of armature winding, magnetic flux per pole and electric load of electric machine, the main dimension relation of permanent magnet machine can be deduced as shown in equation (1) [11].

$$\frac{D^2 l_{ef} n}{P'} = \frac{6.1\times10^{-3}}{\alpha_i K_{Nm} K_{dp} A B_\delta} \tag{1}$$

Where, D is the armature diameter, l_{ef} is the armature length, n is the machine rotating speed, P' is the machine power, α_i is the effective pole arc coefficient, K_{Nm} is the air gap field model coefficient, its value is 1.11 for PMSM, K_{dp} is the armature winding coefficient, A is the ampere conductors along unit

circumference length of armature, B_δ is the air gap flux density. From equation (1), the electric machine constant can be deduced, as shown in equation (2).

$$C_A = \frac{6.1\times10^{-3}}{\alpha_i K_{Nm} K_{dp} A B_\delta} = \frac{D^2 l_{ef}}{P^{'}/n} = \frac{60 D^2 l_{ef}}{2\pi T^{'}} \tag{2}$$

Where, C_A is the electric machine constant, related to the material or cost of electric machine. $T^{'}$ is the electric machine torque.

Energy density can be expressed as equation (3).

$$\sigma = \frac{PT}{m^2} \tag{3}$$

Where, σ is the energy density of electric machine, m is the weight of electric machine and its cooling systems are included, P is the power and T is the torque of electric machine.

2.2 Size design

The high energy density main propulsion machine of electric aircraft can adopt many kinds of slot types, such as pear shaped slot and rectangular slot. In the design of high energy density electric machine, the yoke magnetic density is in the saturation critical state, and the thickness of yoke and tooth can be expressed as equation (4).

$$\begin{cases} h_j = k_j \dfrac{\pi D_{i1} B_\delta}{4 p K_{Fe} B_j} \\ b_t = \dfrac{B_\delta \pi D_{i1} l_{ef}}{Q B_t K_{Fe} l_a} \end{cases} \tag{4}$$

Where, h_j is the stator yoke width, k_j is the stator yoke coefficient, generally in 0.85~0.95, p is the number of pole pairs, K_{Fe} is the stator core superimposed pressure coefficient, B_j is the stator yoke magnetic density, b_t is the stator tooth width, B_t is the stator tooth magnetic density, D_{i1} is the armature diameter, l_a is the core axial length, Q is the stator slot number.

The following equations (5) and (6) can be used for the height and width of permanent magnet of high energy density machine of electric aircraft.

$$h_M = \frac{2 K_s K_a b_{m0} \delta}{(1-b_{m0})\sigma_0} \tag{5}$$

$$b_M = \frac{\sigma_0 B_{\delta 1} \tau_1 L_{ef}}{\pi b_{m0} B_r K_\Phi l_M} \tag{6}$$

Where, K_s is the magnetic saturation coefficient of electric machine, h_M is the magnetization length of permanent magnet, K_a is the rotor correlation coefficient,

b_{m0} is no-load operating point of permanent magnet, δ is the air gap length, B_r is the remanence of permanent magnet, b_M is the width of permanent magnet, $B_{\delta 1}$ is the no-load fundamental wave air gap magnetic density, L_{ef} is the axial length of permanent magnet, K_Φ is the air gap waveform coefficient.

2.3 Loss analysis

At present, it is believed that the loss of permanent magnet machine mainly consists of copper loss of winding, stator core loss, wind wear loss, mechanical friction loss and impurity loss. When designing a high energy density electric machine, it is important to analyze stator iron loss and stator copper loss.

In order to calculate copper loss accurately, the skin effect must be considered. For windings, copper consumption is calculated by equation (7) [12].

$$P_{cu} = m(1 + (k_r + k_s)(\frac{nb}{b_s}\frac{f_s}{50})^2)I_\varphi^2 R_s \tag{7}$$

Where, m is the phase number, k_r is the circulatory coefficient between parallel strands, k_s is eddy current loss coefficient, n is the number of wires in the coil width, b is the coil width, b_s is the groove width, f_s is the frequency, I_φ is the phase current, R_s is the resistance.

For stator core loss, combined with time-step finite element method to determine the magnetic density waveform amplitude of each element, the simple formula method is used to calculate. The core loss per unit mass is determined by looking up table, and the specific calculation equation is shown in (8) [13].

$$\begin{cases} \mathrm{P}_{fe}^{\varepsilon} = K_a p_{1.0/50}^{B_p^e}(B_p^{\varepsilon})^2(\frac{f}{50})^{1.3}\Delta_e L_{ef}\rho_{Fe} \\ \mathrm{P}_{Fe} = \sum_{e=1}^{N_e} \mathrm{P}_{fe}^{\varepsilon} \end{cases} \tag{8}$$

Where, $p_{1.0/50}$ is the iron consumption per unit mass of core lamination when $B = 1\mathrm{T}$ and $f = 50\mathrm{Hz}$, K_a is the empirical coefficient, B_p^e is the magnetic density waveform amplitude of electric machine core unit e, $\mathrm{P}_{fe}^{\varepsilon}$ is the stator core loss of electric machine core unit e, P_{Fe} is the total core loss.

3. Electromagnetic simulation analysis of electric machine

3.1 Basic parameters

With the above electromagnetic design method, a three-phase fractional slot concentrated winding permanent magnet synchronous machine is designed. The electric machine has an embedded structure. And the high permeability iron core and high performance permanent magnet materials are selected to improve

the energy density of propulsion machine. The basic parameters of electric machine designed are shown in table 1.

Table 1

Major parameter of electric machine

Parameters	Numerical value	Parameters	Numerical value
rated power	30kW	outer diameter of stator	215mm
maximum power	40kW	core length	80mm
rated voltage	260V	stator core weight	6.26kg
rated current	140A	rotor core weight	1.37kg
rated frequency	400Hz	winding copper weight	2.85kg
number of pole-pairs	10	permanent magnet weight	1kg
phase number	3	total weight	16.8kg
number of stator slot	21	rated energy density	12.69kW·Nm/kg^2

3.2 Electromagnetic simulation analysis

According to the machine parameters in table 1, the finite element simulation method by ANSYS Maxwell was used to establish the model of the high energy density permanent magnet machine for main propulsion of electric aircraft, as shown in figure 1. The mesh shape of element division adopts triangular shape and the number of units is 56052. The maximum length of elements for permanent magnet is 1 mm and the maximum length of elements for coil is 3mm.

Fig. 2 shows the magnetic density distribution of high energy density permanent magnet machine of main propulsion of electric aircraft under the rated load. The highest magnetic density is located in the teeth and yoke of electric machine, and the highest magnetic density is up to 1.4T, which is close to the saturation of the magnetic density. Therefore, both stator and rotor of electric machine have high material utilization efficiency.

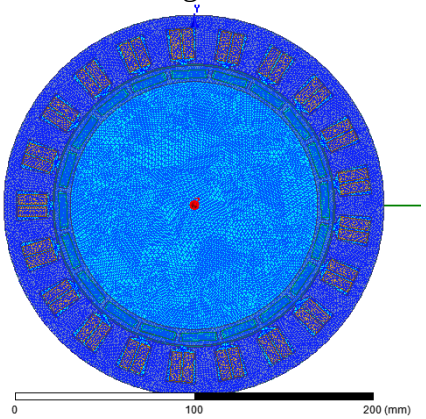

Fig.1 Main propulsion machine model

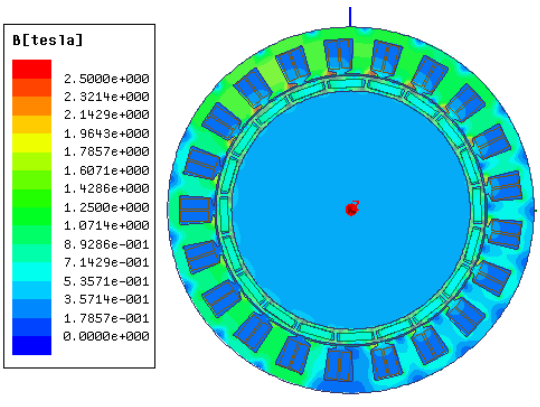

Fig.2 Magnetic flux density distribution

Permanent magnet machine flux represents the relationship between back electromotive force and angular frequency. Figure 3 shows the flux curve of high energy density permanent magnet machine driven by the main propulsion of electric aircraft. It can be seen that the three-phase winding flux of electric machine presents a good sinusoidal state in steady state, and the amplitude of each phase flux reaches 0.1Wb.

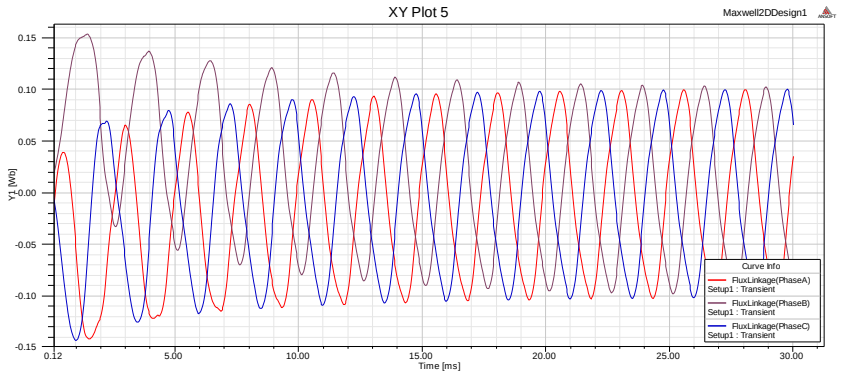

Fig.3 Winding flux linkage

Fig. 4 shows the dynamic torque output curve of high energy density machine for main propulsion of electric aircraft. At rated load, the output torque of main propulsion machine is basically stable at 120Nm after 20ms, which is basically consistent with the theoretical design value.

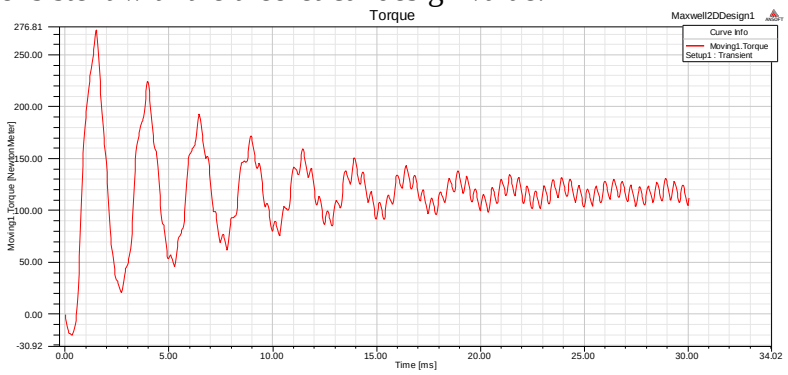

Fig.4 Output torque of electric machine

4. Analysis of mechanical and stress

4.1 Strength check

The strength check of high energy machine is one of the most necessary research points. In terms of strength analysis, it is generally understood that when the force load of a certain part of electric machine reaches its allowable limit value. If the load continues to increase, or there is a strong fluctuation beyond its allowable value, the material will be torn and negative results will emerge.

4.2 Strength simulation analysis

The strength and stress of rotor and shaft of 30kW aviation high energy permanent magnet machine were simulated and analyzed respectively. The software by Simulation software was used to add model, material and load. And the following Simulation images were obtained.

Figure 5 and 6 show the stress distribution of rotor and shaft in the early climbing stage and cruising stage. The initial deformation ratio of climbing stage is 295.32 and the displacement is 0.066~0.48 mm. It can be seen that the deformation ratio in the early cruise stage is 79.50 and the displacement is 0.0047~0.36 mm.

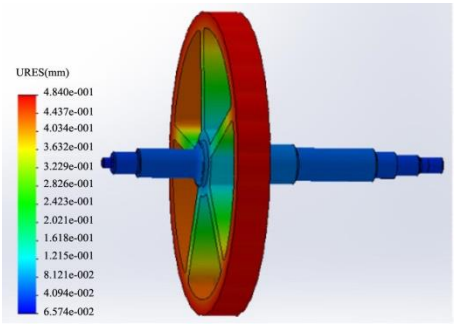

Fig.5 Stress during climbing stage

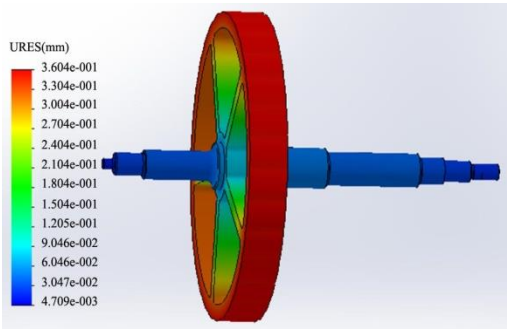

Fig.6 Stress during initial cruise

4.3 Simulation analysis of strength and electromagnetic coupling

When material consumption of electric machine is reduced, its shape variables will increase and electrical parameters will reach saturation under the same load and stress conditions. In order to study the relationship between the size, strength and electromagnetic parameters of electric machine, the strength analysis software and electromagnetic analysis software were combined to obtain the relation distribution diagram of yoke thickness, yoke magnetic density and force shape variables of electric machine as shown in figure 7.

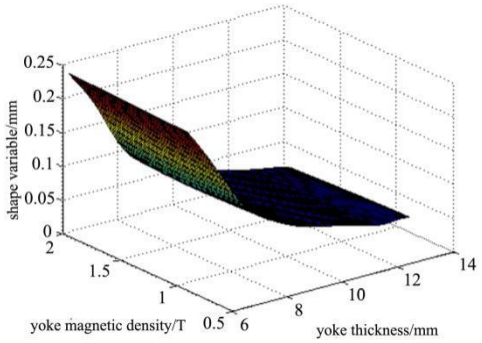

Fig.7 3D relationship among yoke thickness, yoke magnetic density and shape variables

5. Electromagnetic-temperature coupling analysis

5.1 mathematical model

The governing equations of air-fluid mass and momentum are established as shown in equations (9) to (10) [14-15].

$$\frac{\partial \rho}{\partial t} + \nabla \left(\rho V \right) = 0 \tag{9}$$

$$\nabla \left(\rho V \right) = -\nabla p + \nabla \tau + F \tag{10}$$

Where, ρ is the fluid density, t is the time, V is absolute vector velocity, p is the static pressure on the air fluid element, τ is the viscous stresses of fluid molecules, F is the volume force of a fluid element.

For the stator core of the permanent magnet machine, the winding and the cooling medium air, the general energy conservation equation can be calculated by equation (11) below.

$$div(\rho VT) = div(\frac{\lambda}{c} gradT) + S \tag{11}$$

Where, T is the fluid temperature, c is the specific heat at constant pressure of fluid, λ / c is the diffusion coefficient, S is the ratio of the heat energy converted by viscous effect and c.

For a mathematical model of turbulence, the standard $k-\varepsilon$ equation, which is widely used in engineering, is used for modeling, as shown in equation (12).

$$\begin{cases} \dfrac{\partial(\rho k)}{\partial t} + \mathrm{div}(\rho k V) = \mathrm{div}[(\mu + \dfrac{\mu_t}{\sigma_k})\mathrm{grad} k] + G_k - \rho\varepsilon \\ \dfrac{\partial(\rho \varepsilon)}{\partial t} + \mathrm{div}(\rho \varepsilon V) = \mathrm{div}[(\mu + \dfrac{\mu_t}{\sigma_\varepsilon})\mathrm{grad}\varepsilon] + G_{1\varepsilon}\dfrac{\varepsilon}{k} G_k - G_{2\varepsilon}\rho\dfrac{\varepsilon^2}{k} \end{cases} \tag{12}$$

Where, k is the turbulent kinetic energy, ε is the spreading factor, μ is the dynamic viscosity, G_k is the turbulence generation rate, μ_t is the turbulent viscosity coefficient, $G_{1\varepsilon}$ and $G_{2\varepsilon}$ is constant, σ_k and σ_ε is the Turbulent Planck constant.

5.2 Electromagnetic temperature simulation analysis

For electromagnetic thermal coupling analysis of high energy density permanent magnet machine, the multi-software simulation analysis method is adopted. For electromagnetic temperature coupling of electric machine, a coupling analysis can be used between Maxwell and Workbench to calculate electric machine loss and temperature rise distribution.

Through the simulation analysis, the heat flux distribution image of a steady-state tangent plane of main propulsion machine can be obtained, as shown in Fig. 8.

Because the thermal load of high energy density machine is different under different working power, the temperature distribution of high energy density machine under different thermal load can be analyzed. After several simulations, the temperature rise trend of the 30kW permanent magnet machine designed in this paper under different thermal loads can be obtained, as shown in figure 9. With the increase of thermal load, the temperature rise of winding and shell keeps rising. When the thermal load of machine is 6500A^2/(cm·mm^2), the temperature rise of winding is 125.7K and that of shell is 96.7K. Under the rated power, if its temperature appreciation exceeds its insulation margin, then the electric machine size should be redesigned or the thermal load should be reduced.

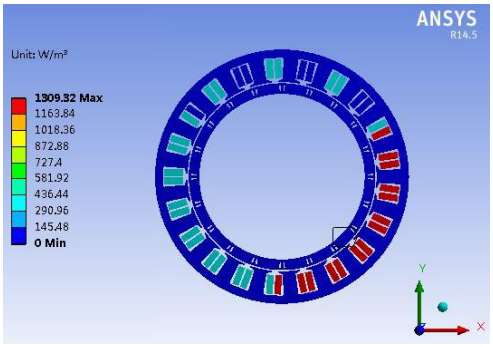

Fig.8 Model of Maxwell-Fluent

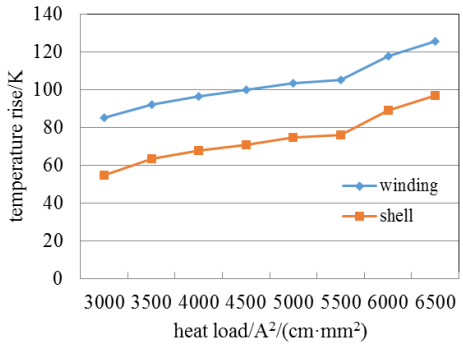

Fig.9 Temperature rise trend

6. Experimental Analysis

6.1 prototype development

The rated power of prototype is 30kW, the rated speed is 2400 r/min, and the rated energy density is 8.96 kW·N·m/kg^2. The mechanical structure of enclosed stator and hollow rotor is adopted. The open structure of permanent magnet machine can effectively improve the heat dissipation capacity, so as to fully improve the energy density index of the system and maximize the performance of main propulsion system. The developed prototype is shown in Fig. 10.

Fig.10 Experimental prototype

6.2 experiment platform

For the back EMF measurement of high energy density permanent magnet machine for all-electric aircraft, the method of double machine towing as shown in figure 11 is adopted. The average measured value of back EMF is 219.5V.

Fig.11 Towing experiment platform

The load of the main propulsion machine is propeller. When the main propulsion machine is in normal operation, the propeller load will generate high speed forced cooling wind speed behind, which plays a good role in the heat dissipation of electric machine. Figure 12 shows a tower-mounted test platform for aviation system, which mainly consists of main propulsion machine, torque and speed measuring instrument, temperature sensor, propeller and power supply.

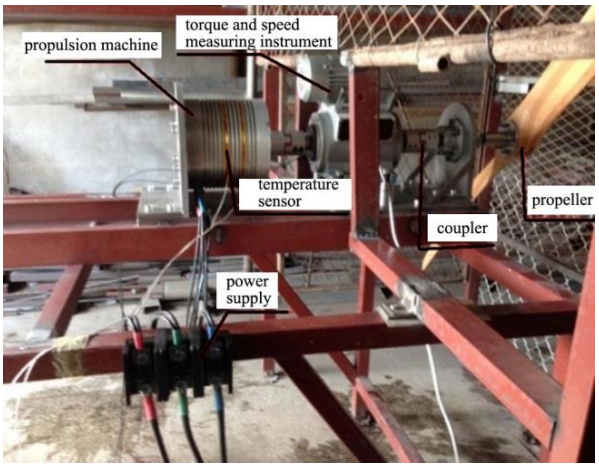

Fig.12 Propeller test platform

The above experimental platform was used to complete the no-load and load data of the main propulsion machine, in which the maximum speed reached 2600r/min during no-load phase. When the propeller is loaded, the propeller is 1.6m long, the maximum speed is 2400r/min, and the maximum output power is 38.6kw. Figure 13~16 show specific experimental data respectively. The energy

density of conventional permanent magnet machine is less than 5 kW·N·m/kg^2, and the experiment shows that the maximum energy density of electric machine designed is 21kW·N·m/kg^2, which is 4.2 times more than that of the former.

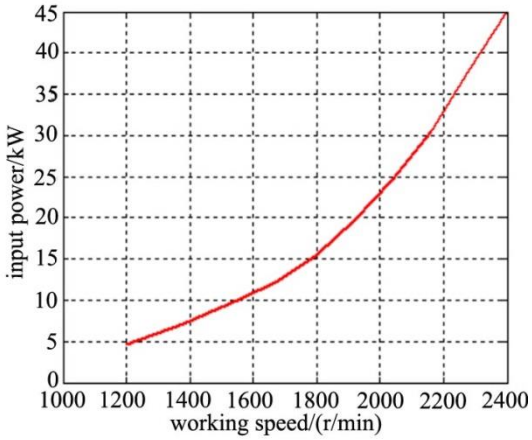

Fig.13 Actual speed and input power curve

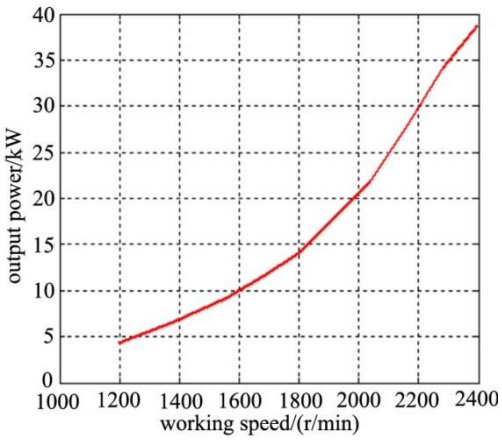

Fig.14 Actual speed and output power curve

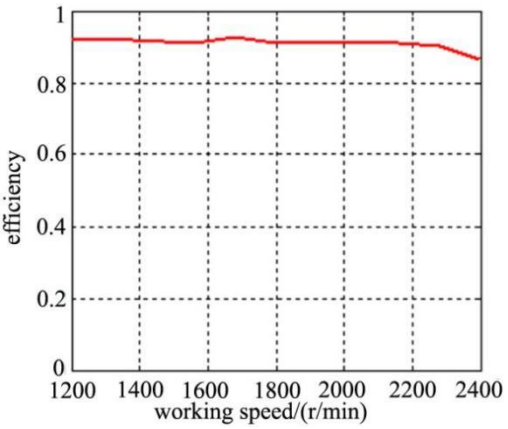

Fig.15 Actual speed and efficiency curve

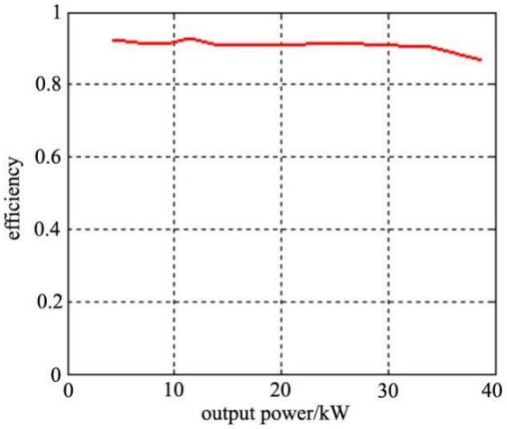

Fig.16 Output power and efficiency curve

The above experimental data show that the performance parameters of high energy density permanent magnet machine have reached the requirements of main propulsion power system, and the permanent magnet machine designed and developed has a high energy density.

7. Conclusions

Taking permanent magnet machine as research object and combining its working characteristics, this paper presents a novel approach, which can be used for improving energy density of electric machine of all-electric aircraft based on

the multi-physical field analysis. The multi-physical field simulation and experimental verification are carried out and the following conclusions are drawn.

1) The general design method of high energy density permanent magnet machine is present, and the energy density of main propulsion electric machine of all electric aircraft is proposed by multi-physical field analysis method.

2) The definition of high energy density index of permanent magnet machine is shown on and the size design formula of high energy density permanent magnet machine and the loss calculation method are offered.

3) The mechanical and stress field analysis of high energy density permanent magnet machine is studied. The numerical relationship of yoke thickness, yoke magnetic density and force shape variables of electric machine is described clearly.

4) The electromagnetic-temperature coupling analysis method of high energy density permanent magnet machine is presented. When electric machine is in the state of maximum thermal load and the temperature rise conforms to its insulation grade, it is qualified, otherwise it needs to be redesigned.

Acknowledgement

The study was funded by the National Natural Science Foundation of China (51607115), the National Natural Science Foundation of China (61941305) and the Tianjin Science and Technology Project (19YFFCYS00110). The authors also wish to thank those people who provided extensive assistance, but whose names are not listed in the paper.

R E F E R E N C E S

[1]. *E. Ganev*. "Selecting the Best Electric Machines for Electrical Power-Generation Systems: High-performance solutions for aerospace More electric architectures". IEEE Electrification Magazine, **vol. 2**, no. 4, Apr. 2014, pp. 13-22.

[2]. *P. Ragot , M. Markovic , Y. Perriard*. "Optimization of Electric Motor for a Solar Airplane Application". IEEE Transactions on Industry Applications, **vol. 42**, no. 4, Apr. 2006, pp. 1053-1061.

[3]. *D. Cervinka, J. Knobloch, P. Prochazka*, et al. "Electric powered airplane VUT 051 RAY". 16th International Conference on Mechatronics - Mechatronika (ME), Brno, 2014.

[4]. *W. Cao, B.C. Mecrow, G.J. Atkinson*, et al. "Overview of electric motor technologies used for more electric aircraft (MEA)". IEEE transactions on industrial electronics, **vol. 59**, no. 9, Sept. 2011, pp. 3523-3531.

[5]. *P.J. Masson, C.A. Luongo*. "High power density superconducting motor for all-electric aircraft propulsion". IEEE Transactions on Applied Superconductivity, **vol. 15**, no. 2, Feb. 2005, pp. 2226-2229.

[6]. *S. De, M. Rajne, S. Poosapati*, et al. "Low-inductance axial flux BLDC motor drive for more electric aircraft". IET Power Electronics, **vol. 5**, no. 1, Jan. 2012, pp. 124-133.

[7]. *S.T. Lee*, *H.J. Kim*, *J. Cho*. "Thermal analysis of interior permanent-magnet synchronous motor by electromagnetic field-thermal linked analysis". Journal of Electrical Engineering and Technology, **vol. 7**, no. 6, Jun. 2012, pp. 905-910.

[8]. *Z. Tan*, *X.G. Song*, *B. Ji*, et al. "3D thermal analysis of a permanent magnet motor with cooling fans". Journal of Zhejiang University SCIENCE A, **vol. 16**, no. 8, Aug. 2015, pp. 616-621.

[9]. *J.D. Widmer*, *C.M. Spargo*, *G.J. Atkinson*, et al. "Solar plane propulsion motors with precompressed aluminum stator windings". IEEE Transactions on Energy Conversion, **vol. 29**, no. 3, Jul. 2014, pp. 681-688.

[10]. *V. Iosif*, *D. Roger*, *S. Duchesne*, et al. "Assessment and improvements of inorganic insulation for high temperature low voltage motors". IEEE Transactions on Dielectrics and Electrical Insulation, **vol. 23**, no. 5, Oct. 2016, pp. 2534-2542.

[11]. *R.Y. Tang*. Modern permanent magnet machines theory and design. China Machine Press, Beijing, 1997.

[12]. *Jibin Zhang*, *Hongliang Zou*, *Xia Chen*, et al. "Analysis of 3D Transient Temperature Field for Torque Motor in the State of Steady Electromagnetic Field". Proceedings of The Chinese Society for Electrical Engineering, **vol. 27**, no. 21, Jul. 2007, pp. 66-70.

[13]. *Xiaoguang Kong*, *Fengxiang Wang*, *Yunlong Xu*, et al. "Analysis and calculation of iron losses of high-speed permanent magnet machines". Electric Machine and Control, **vol. 14**, no. 9, Sep. 2010, pp. 26-30.

[14]. *Qingsheng Zhou*, *Surong Huang*, *Qi Zhang*, et al. "Temperature Field Analysis of Novel Cooling Structure Ultra-precision Planar Motor". Proceedings of The Chinese Society for Electrical Engineering, **vol. 32**, no. 15, May. 2012, pp. 134-139.

[15]. *Bingyi Zhang*, *Sen Wang*, *Guihong Feng*. "Temperature field research for main propulsion motor of unmanned aerial vehicle based on fluid-solid coupled theory". Electric Machines and Control, **vol. 18**, no. 6, Jul. 2014, pp. 116-120.